

Multiphoton coherent population oscillation

A. V. Sharypov

*Kirensky Institute of Physics, 50 Akademgorodok, Krasnoyarsk, 660036, Russia and
Siberian Federal University, 79 Svobodny Ave., Krasnoyarsk, 660041, Russia*

A. D. Wilson-Gordon

Department of Chemistry, Bar-Ilan University, Ramat Gan 52900, Israel

We study the bichromatic driving of a two-level system which displays long-lived coherent population oscillations (CPO). We show that under certain conditions, multiphoton parametric interaction leads to the appearance of CPO resonances at the subharmonic frequencies. In addition, in the region of the CPO resonances, there is strong parametric interaction between the weak sideband components of the electromagnetic field.

PACS numbers: 42.50.Gy, 42.50.Hz, 42.65.Yj

I. INTRODUCTION

Non-linear interaction between electromagnetic fields can lead to the appearance of resonances with a bandwidth which is much narrower than the unperturbed natural linewidth. The most familiar effects that can give such narrowband response are electromagnetically induced transparency (EIT) [1] and coherent population oscillations (CPO) [2]. In the EIT and CPO cases, the strong pump can form a transparency window in the probe absorption spectrum accompanied by steep dispersion of the refractive index that leads to effects such as slow light [3, 4]. The narrowband medium response can also appear in the four-wave mixing (FWM) process [5], leading under certain conditions to narrowband biphoton generation due to EIT [6, 7] or CPO [8]. Although there are similarities between EIT and CPO, these effects are actually different in nature, and the properties of the non-linear response in each case are determined by different system parameters. For example, in the case of EIT, the minimal bandwidth of the resonance is determined by the transverse relaxation rate of the two-photon transition, whereas in the case of CPO, the minimal bandwidth is determined by the effective longitudinal relaxation rate; in the EIT case, the resonance appears at zero two-photon detuning, whereas in the CPO case, the non-linear resonance is centered at the pump frequency. The fact that in the CPO case, the weak signal is always centered at the pump frequency makes it difficult to filter out the weak signal from the strong pump and incoherent scattering.

Here, we analyze the response of a two-level system (TLS) that displays long-lived coherent population oscillations in the presence of a bichromatic pump, and one or two weak fields. The two sidebands of the pump are symmetrically displaced from the pump frequency ω_0 and in the case where the scanning is realized by two probe fields, these fields are also symmetrically displaced from ω_0 (see Fig. 1). The interaction of the TLS with a polychromatic field has been studied from many different aspects; see, for example, [9] and references therein. In the bichromatic fields, resonances at the subharmonic

frequencies $\omega_{sub} = \omega_0 \pm (2n + 1)\delta$ [10, 11] appear where δ is the frequency difference between the two pumps and n is an integer. Here we demonstrate that these resonances can appear under CPO conditions with a width determined by the effective longitudinal relaxation rate. We also demonstrate that there is effective parametric interaction between two weak probes tuned in the region of the two symmetrically displaced CPO resonances. Under certain conditions this parametric interaction can appear at a pump Rabi frequency well below the transverse relaxation rate of the TLS.

II. THE MODEL

Let us consider the two-level quantum system composed of levels $|1\rangle$ and $|2\rangle$ interacting with the electromagnetic field E . It is assumed that system has an additional off-resonant quantum metastable state $|m\rangle$ which is radiatively coupled to the TLS (see Fig. 1). The set of Bloch equations for the present system has the following form:

$$\left(\frac{d}{dt} + \Gamma_{21} + i\omega_{21}\right)\rho_{21} + iV_{21}(\rho_{11} - \rho_{22}) = 0 \quad (1)$$

$$\left(\frac{d}{dt} + \Gamma_{21} - i\omega_{21}\right)\rho_{12} - iV_{12}(\rho_{11} - \rho_{22}) = 0 \quad (2)$$

$$V_{12}\rho_{21} - iV_{21}\rho_{12} + \frac{d\rho_{11}}{dt} - \gamma_{21}\rho_{22} - \gamma_m\rho_m = 0 \quad (3)$$

$$\frac{d\rho_m}{dt} + \gamma_m\rho_m - \gamma_o\rho_{22} = 0 \quad (4)$$

where V_{21} is the total Rabi frequency, and Γ_{21} is the transverse relaxation rate of the $|2\rangle - |1\rangle$ transition, and γ_{21} , γ_o , and γ_m are the population relaxation constants from the excited state to the ground state, from the excited state to the metastable state, and from the

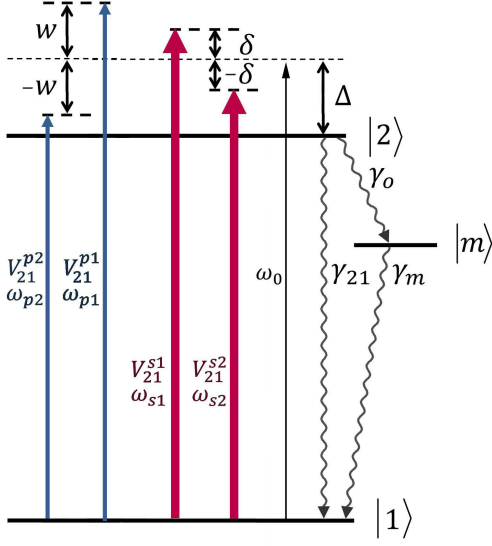


FIG. 1: A two-level system $|2\rangle - |1\rangle$ interacting with bichromatic pump field $V_{21}^{s1,s2}$ and bichromatic probe field $V_{21}^{p1,p2}$. γ_{21} longitudinal relaxation from the excited state to the ground, γ_o - longitudinal relaxation rate from the excited state to the intermediate metastable state $|m\rangle$ and γ_m is the longitudinal relaxation rate from intermediate state to the ground.

metastable to the ground state, respectively. Further, we assume that the system is closed and that the total population in the system is conserved so that

$$\rho_{11} + \rho_{22} + \rho_m = 1. \quad (5)$$

Let us introduce the population inversion

$$r = \rho_{22} - \rho_{11}, \quad (6)$$

and, using Eqs. (5) and (6), define ρ_{11} and ρ_{22} in terms of r and ρ_m . We then rewrite Eqs. (1) - (4) and obtain the following set of equations:

$$\left(\frac{d}{dt} + \Gamma_{21} + i\omega_{21} \right) \rho_{21} - iV_{21}r = 0, \quad (7)$$

$$\left(\frac{d}{dt} + \Gamma_{21} - i\omega_{21} \right) \rho_{12} + iV_{12}r = 0, \quad (8)$$

$$2iV_{12}\rho_{21} - 2iV_{21}\rho_{12} - \left(\frac{dr}{dt} + \gamma_{21} + \frac{\gamma_o}{2} \right) r + \left(\gamma_{21} - \gamma_m + \frac{\gamma_o}{2} \right) \rho_m = \gamma_{21} + \frac{\gamma_o}{2}, \quad (9)$$

$$-\frac{\gamma_o}{2}r + \left(\frac{d}{dt} + \gamma_m + \frac{\gamma_o}{2} \right) \rho_m = \frac{\gamma_o}{2}. \quad (10)$$

A. The electromagnetic field

We now specify the electromagnetic fields acting on the system. We consider the case of the bichromatic pumping of the TLS at frequencies ω_{s1} and ω_{s2} , and define the detuning of the pump fields from resonance in the following way

$$\Delta = \omega_0 - \omega_{21}, \quad (11)$$

where $\omega_0 = (\omega_{s1} + \omega_{s2})/2$ and ω_{21} is the resonance frequency of the $|1\rangle \rightarrow |2\rangle$ transition. We also apply a weak probe field which is a combination of two sidebands arranged symmetrically with respect to ω_0 with frequencies ω_{p1} and ω_{p2} . The Rabi frequency for the total electromagnetic field can be written in the form

$$V_{21} = \left(V_{21}^{s1} e^{-i\delta t} + V_{21}^{s2} e^{i\delta t} + V_{21}^{p1} e^{-i\omega t} + V_{21}^{p2} e^{i\omega t} \right) e^{-i\omega_0 t}, \quad (12)$$

where V_{21}^{s1} , V_{21}^{s2} , V_{21}^{p1} , and V_{21}^{p2} are the Rabi frequencies of the corresponding fields. We also define the following detunings:

$$\delta = \omega_{s1} - \omega_0 = -(\omega_{s2} - \omega_0), \quad w = \omega_{p1} - \omega_0 = -(\omega_{p2} - \omega_0). \quad (13)$$

Next we move to the frame rotating at frequency ω_0 and define

$$\sigma_{21} = \rho_{21} e^{i\omega_0 t}, \quad \sigma_{12} = \rho_{12} e^{-i\omega_0 t}, \quad \sigma_0 = r, \quad \sigma_m = \rho_{mm}. \quad (14)$$

Substituting Eqs. (12) and (14) into Eqs. (7)-(10), we obtain a set of equations which we write in the matrix form

$$BS = F, \quad (15)$$

where

$$S = \begin{pmatrix} \sigma_{21} \\ \sigma_{12} \\ \sigma_0 \\ \sigma_m \end{pmatrix}, \quad F = \begin{pmatrix} 0 \\ 0 \\ -(\gamma_{21} + \frac{\gamma_o}{2}) \\ \frac{\gamma_o}{2} \end{pmatrix}, \quad (16)$$

and the matrix B is written as the sum of components oscillating at the different frequencies

$$B = O + D^{+\delta} e^{i\delta t} + D^{-\delta} e^{-i\delta t} + W^{+w} e^{i\omega t} + W^{-w} e^{-i\omega t}, \quad (17)$$

where the matrices are defined as

$$O = \frac{d}{dt} I + \begin{pmatrix} \Gamma_{21} - i\Delta & 0 & 0 & 0 \\ 0 & \Gamma_{21} + i\Delta & 0 & 0 \\ 0 & 0 & \gamma_{21} + \frac{\gamma_o}{2} & \gamma_m - \frac{\gamma_o}{2} - \gamma_{21} \\ 0 & 0 & -\frac{\gamma_o}{2} & \gamma_m + \frac{\gamma_o}{2} \end{pmatrix}, \quad (18)$$

$$D^{-\delta} = i \begin{pmatrix} 0 & 0 & -V_{21}^{s1} & 0 \\ 0 & 0 & V_{12}^{s2} & 0 \\ -2V_{12}^{s2} & 2V_{21}^{s1} & 0 & 0 \\ 0 & 0 & 0 & 0 \end{pmatrix}, \quad (19)$$

$$D^{+\delta} = i \begin{pmatrix} 0 & 0 & -V_{21}^{s2} & 0 \\ 0 & 0 & V_{12}^{s1} & 0 \\ -2V_{12}^{s1} & 2V_{21}^{s2} & 0 & 0 \\ 0 & 0 & 0 & 0 \end{pmatrix}, \quad (20)$$

$$W^{-w} = i \begin{pmatrix} 0 & 0 & -V_{21}^{p1} & 0 \\ 0 & 0 & V_{12}^{p2} & 0 \\ -2V_{12}^{p2} & 2V_{21}^{p1} & 0 & 0 \\ 0 & 0 & 0 & 0 \end{pmatrix}, \quad (21)$$

$$W^{+w} = i \begin{pmatrix} 0 & 0 & -V_{21}^{p2} & 0 \\ 0 & 0 & V_{12}^{p1} & 0 \\ -2V_{12}^{p1} & 2V_{21}^{p2} & 0 & 0 \\ 0 & 0 & 0 & 0 \end{pmatrix}, \quad (22)$$

and I is the identity matrix of order 4.

B. Expansion of the solution

As can be seen from Eq. (17), the Hamiltonian of the system has a periodic time dependence with two characteristic frequencies δ and w . In order to find a solution, we use the Floquet theorem and make a harmonic expansion of the vector of the density-matrix elements S

$$S = \sum_{n=-\infty}^{+\infty} \sum_{m=-\infty}^{+\infty} S^{n,m} e^{i(n\delta + mw)t}. \quad (23)$$

After substituting Eq. (23) into Eq. (15), we take the time derivative of the oscillating term and separate the equations with different time dependence to obtain the matrix recurrence relation

$$(O + T) S^{n,m} + D^{-\delta} S^{n+1,m} + D^{+\delta} S^{n-1,m} + W^{-w} S^{n,m+1} + W^{+w} S^{n,m-1} = F \delta_{n=0,m=0}, \quad (24)$$

where

$$T = i(n\delta + mw) I. \quad (25)$$

C. Steady state approximation

We now make the steady-state approximation and rewrite the matrix equation of Eq. (24) as a set of four algebraic equations:

$$\begin{aligned} \sigma_{21}^{n,m} &= i P_{21}^{n,m} \\ (V_{21}^{s1} \sigma_0^{n+1,m} + V_{21}^{s2} \sigma_0^{n-1,m} + V_{21}^{p1} \sigma_0^{n,m+1} + V_{21}^{p2} \sigma_0^{n,m-1}), \end{aligned} \quad (26)$$

$$\begin{aligned} \sigma_{12}^{n,m} &= -i P_{12}^{n,m} \\ (V_{12}^{s2} \sigma_0^{n+1,m} + V_{12}^{s1} \sigma_0^{n-1,m} + V_{12}^{p1} \sigma_0^{n,m-1} + V_{12}^{p2} \sigma_0^{n,m+1}), \end{aligned} \quad (27)$$

$$\begin{aligned} & \left[\gamma_{21} + \frac{\gamma_o}{2} + i(n\delta + mw) \right] \sigma_0^{n,m} - \left(\gamma_{21} - \gamma_m + \frac{\gamma_o}{2} \right) \sigma_m^{n,m} \\ & 2iV_{21}^{s1} \sigma_{12}^{n+1,m} - 2iV_{12}^{s1} \sigma_{21}^{n-1,m} - 2iV_{12}^{s2} \sigma_{21}^{n+1,m} + \\ & 2iV_{21}^{s2} \sigma_{12}^{n-1,m} + 2iV_{21}^{p1} \sigma_{12}^{n,m+1} - 2iV_{12}^{p1} \sigma_{21}^{n,m-1} + \\ & 2iV_{21}^{p2} \sigma_{12}^{n,m-1} - 2iV_{12}^{p2} \sigma_{21}^{n,m+1} = - \left(\gamma_{21} + \frac{\gamma_o}{2} \right) \delta_{n=0,m=0}, \end{aligned} \quad (28)$$

$$\sigma_m^{n,m} = P_m^{n,m} (\delta_{n=0,m=0} + \sigma_0^{n,m}), \quad (29)$$

where

$$P_{21}^{n,m} = [\Gamma_{21} + i\Delta + i(n\delta + mw)]^{-1}, \quad (30)$$

$$P_{12}^{n,m} = [\Gamma_{21} - i\Delta + i(n\delta + mw)]^{-1}, \quad (31)$$

$$P_m^{n,m} = \frac{\gamma_o}{2} \left[\gamma_m + \frac{\gamma_o}{2} + i(n\delta + mw) \right]^{-1}. \quad (32)$$

We now solve these equations by writing an equation for the function $\sigma_0^{m,n}$ alone. Substituting corresponding terms from Eqs. (26), (27), and (29) into Eq. (28), we obtain a two-dimensional recurrence relation for $\sigma_0^{m,n}$

$$\begin{aligned} & a_{n,m}^1 \sigma_0^{n,m} + a_{n,m}^2 \sigma_0^{n-2,m} + a_{n,m}^3 \sigma_0^{n+2,m} + a_{n,m}^4 \sigma_0^{n-1,m-1} + \\ & a_{n,m}^5 \sigma_0^{n+1,m-1} + a_{n,m}^6 \sigma_0^{n-1,m+1} + a_{n,m}^7 \sigma_0^{n+1,m+1} + \\ & a_{n,m}^8 \sigma_0^{n,m+2} + a_{n,m}^9 \sigma_0^{n,m-2} = -R_{0,0} \delta_{n=0,m=0}, \end{aligned} \quad (33)$$

where we have introduced the following notation:

$$\begin{aligned} a_{n,m}^1 &= 2 |V_{21}^{s1}|^2 (P_{21}^{n-1,m} + P_{12}^{n+1,m}) + \\ & 2 |V_{21}^{s2}|^2 (P_{21}^{n+1,m} + P_{12}^{n-1,m}) + \\ & 2 |V_{21}^{p1}|^2 (P_{21}^{n,m-1} + P_{12}^{n,m+1}) + \\ & 2 |V_{21}^{p2}|^2 (P_{21}^{n,m+1} + P_{12}^{n,m-1}) + R_{n,m}, \end{aligned} \quad (34)$$

$$a_{n,m}^2 = 2V_{12}^{s1} V_{21}^{s2} (P_{21}^{n-1,m} + P_{12}^{n-1,m}), \quad (35)$$

$$a_{n,m}^3 = 2V_{21}^{s1} V_{12}^{s2} (P_{21}^{n+1,m} + P_{12}^{n+1,m}), \quad (36)$$

$$\begin{aligned} a_{n,m}^4 &= 2V_{21}^{s2} V_{12}^{p1} (P_{21}^{n,m-1} + P_{12}^{n-1,m}) + \\ & 2V_{12}^{s1} V_{21}^{p2} (P_{21}^{n-1,m} + P_{12}^{n,m-1}), \end{aligned} \quad (37)$$

$$\begin{aligned} a_{n,m}^5 &= 2V_{21}^{s1} V_{12}^{p1} (P_{21}^{n,m-1} + P_{12}^{n+1,m}) + \\ & 2V_{12}^{s2} V_{21}^{p2} (P_{21}^{n+1,m} + P_{12}^{n,m-1}), \end{aligned} \quad (38)$$

$$a_{n,m}^6 = 2V_{12}^{s1}V_{21}^p \left(P_{21}^{n-1,m} + P_{12}^{n,m+1} \right) + 2V_{21}^{s2}V_{12}^{p2} \left(P_{21}^{n,m+1} + P_{12}^{n-1,m} \right), \quad (39)$$

$$a_{n,m}^7 = 2V_{12}^{s2}V_{21}^{p1} \left(P_{21}^{n+1,m} + P_{12}^{n,m+1} \right) + 2V_{21}^{s1}V_{12}^{p2} \left(P_{21}^{n,m+1} + P_{12}^{n+1,m} \right), \quad (40)$$

$$a_{n,m}^8 = 2V_{21}^{p1}V_{12}^{p2} \left(P_{21}^{n,m+1} + P_{12}^{n,m+1} \right), \quad (41)$$

$$a_{n,m}^9 = 2V_{12}^{p1}V_{21}^{p2} \left(P_{21}^{n,m-1} + P_{12}^{n,m-1} \right), \quad (42)$$

$$R_{n,m} = \gamma_{21} + \frac{\gamma_o}{2} + i(n\delta + mw) - P_m^{n,m} \left(\gamma_{21} - \gamma_m + \frac{\gamma_o}{2} \right). \quad (43)$$

The recurrence relation of Eq. (33) is solved numerically and allows us to treat probe fields of arbitrary strength.

D. Polarization

The medium polarization is determined by the non-diagonal matrix element

$$P(t) = \mu N (\rho_{21} + c.c.) = \mu N \left(\sum_{n=-\infty}^{+\infty} \sum_{m=-\infty}^{+\infty} \sigma_{21}^{n,m} e^{-i\omega_0 t} e^{i(n\delta + mw)t} + c.c. \right). \quad (44)$$

Thus the component of the polarization that oscillates at a particular frequency gives the medium's response to the electromagnetic field at this frequency. As can be seen from Eq. (44), the polarization at the probe frequency ω_{p1} is proportional to $\sigma_{21}^{0,-1}$ which can be found from Eq. (26)

$$\sigma_{21}^{0,-1} = iP_{21}^{0,-1} \left(V_{21}^{s1}\sigma_0^{1,-1} + V_{21}^{s2}\sigma_0^{-1,-1} + V_{21}^{p1}\sigma_0^{0,0} + V_{21}^{p2}\sigma_0^{0,-2} \right). \quad (45)$$

In the next section we analyze the normalized probe absorption, which is defined as $\alpha/\alpha_0 = -\text{Im} \sigma_{21}^{0,-1} \Gamma_{21}/V_{21}^{p1}$, for several cases.

III. THE CPO RESONANCE IN MONOCHROMATIC PUMPING

The role of the excited-state decay's branching ratio to the ground and metastable states is not discussed in the literature. However, it is of crucial importance in obtaining CPO at the subharmonic frequencies. Thus,

in order to better understand the behavior of the system in a bichromatic driving field, we first consider the case of a monochromatic driving where it is easy to get an analytical result and analyze the role of the branching ratio. Let us consider the interaction of the TLS with a strong pump and a weak probe. In this case, we take $V_{21}^{s2} = V_{21}^{p2} = 0$ in Eq. (45) so that

$$\sigma_{21}^{0,-1} = iP_{21}^{0,-1} \left(V_{21}^{s1}\sigma_0^{1,-1} + V_{21}^{p1}\sigma_0^{0,0} \right). \quad (46)$$

Assuming that the probe field is weak we can keep only the first-order terms in the probe Rabi frequencies. We then obtain for the functions $\sigma_0^{1,-1}$ and $\sigma_0^{0,0}$ of Eq. (33)

$$\sigma_0^{1,-1} = -\frac{a_{1,-1}^6}{a_{1,-1}^1} \sigma_0^{0,0}, \quad (47)$$

$$\sigma_0^{0,0} = -R_{0,0}/a_{0,0}^1 = -\left(1 - \frac{\kappa}{1+\kappa} \right), \quad (48)$$

where

$$\kappa = \kappa_{TLS} (\gamma_0/2\gamma_m + 1) \quad (49)$$

is the saturation parameter of the system and

$$\kappa_{TLS} = 4 \frac{|V_{12}^{1s}|^2}{\gamma_2 \Gamma_{21}} \frac{1}{1 + \Delta_s^2/\Gamma_{21}^2} \quad (50)$$

is the saturation parameter of the ordinary two-level system (if there is no additional channel for the decay via intermediate state). The functions $a_{1,-1}^1$ and $a_{1,-1}^6$ are found from Eqs. (34) and (39) to be

$$a_{1,-1}^1 = \frac{[\gamma_2 - i\Delta_p][\gamma_m - i\Delta_p]}{\gamma_m + \gamma_o/2 - i\Delta_p} + 4|V_{21}^{s1}|^2 \frac{\Gamma_{21} - i\Delta_p}{[\Gamma_{21} + i(\Delta_s + \Delta_p)][\Gamma_{21} - i(\Delta_s - \Delta_p)]}, \quad (51)$$

$$a_{1,-1}^6 = 4V_{12}^0 V_{21}^{p1} \frac{\Gamma_{21} + i(\Delta_s - \Delta_p)/2}{(\Gamma_{21} + i\Delta_s)(\Gamma_{21} - i\Delta_p)}, \quad (52)$$

where for convenience we have introduced the pump detuning from resonance $\Delta_s \equiv \Delta - \delta = \omega_{s1} - \omega_{21}$ and pump-probe detuning $\Delta_p \equiv \omega - \delta = \omega_{p1} - \omega_{s1}$.

We are interested in the shape of the narrow dip centered at the pump frequency and associated with the CPO effect. This structure has a characteristic bandwidth of the order of γ_m which is much less than the natural bandwidth of the transition from the excited to the ground state as the level $|m\rangle$ is assumed to be metastable. Thus, in Eqs. (51) and (52), we use the approximation

$$\gamma_m, \Delta_p \ll \Gamma_{21}, \gamma_2 \quad (53)$$

and obtain

$$\frac{a_{1,-1}^6}{a_{1,-1}^1} \approx 4 \frac{V_{12}^{s1} V_{21}^{p1}}{\gamma_2 \Gamma_{21} (1 + \Delta_s^2 / \Gamma_{21}^2)} \frac{S}{1 + \kappa_{TLS}} \frac{\gamma_m + \gamma_0/2 - i\Delta_p}{(W - i\Delta_p)}, \quad (54)$$

where W is the bandwidth of the CPO dip

$$W = \gamma_m \frac{1 + \kappa}{1 + \kappa_{TLS}}. \quad (55)$$

and the parameter $S \equiv (1 + \Delta_s^2 / 2\Gamma_{21}^2 - i\Delta_s / 2\Gamma_{21})$. Combining Eqs. (47), (48), and (54), we obtain the medium response at the probe frequency in the region of the CPO resonance

$$\sigma_{21}^{0,-1} = \frac{-iV_{21}^{p1}}{1 + \kappa} \frac{1}{\Gamma_{21} + i(\Delta_s - \Delta_p)} (1 - XS), \quad (56)$$

where the first term in the brackets determines the saturation of the system due to the pump and the second term X includes the coherent interaction between pump and probe fields

$$X = 1 - \frac{1}{1 + \kappa_{TLS}} \frac{\gamma_m - i\Delta_p \kappa_{TLS}}{W - i\Delta_p}. \quad (57)$$

Further, for simplicity we consider the case of small pump detunings and assume that $S \approx 1$.

Bandwidth The bandwidth of the resonance is determined by the function W [see Eq. (55)]. In the case of the “classical” CPO, for which $\gamma_2 \approx \gamma_0 \gg \gamma_m$, we have $\kappa \gg \kappa_{TLS}$, so that in the denominator of Eq. (55) we can omit κ_{TLS} and obtain the same result as in [12]

$$W = \gamma_m (1 + \kappa). \quad (58)$$

Thus the minimal bandwidth of the CPO resonance is determined by γ_m and this resonance experiences power broadening. In the opposite case for which $\gamma_2 \gg \gamma_0 \approx \gamma_m$, κ and κ_{TLS} are of the same order. In this case, the bandwidth experiences fast saturation

$$W = \gamma_m + \frac{\gamma_0}{2} \frac{\kappa_{TLS}}{1 + \kappa_{TLS}} \quad (59)$$

and will not exceed $\gamma_m + \frac{\gamma_0}{2}$.

Depth The depth is determined from Eq. (56) by putting $\Delta_p = 0$. We obtain $\alpha(\Delta_p = 0)/\alpha_0 = 1/(1 + \kappa)^2$.

Amplitude From Eq. (56), we can determine the amplitude of the CPO dip. The dip itself comes from the multiplier $(\gamma_m - i\Delta_p \kappa_{TLS})/(W - i\Delta_p)$ in Eq. (57). Its amplitude α_a is given by the difference between Eq. (56) with and without this term at point $\Delta_p = 0$

$$\alpha_a = \frac{\kappa}{(1 + \kappa)^2} \frac{\gamma_0/2\gamma_m}{\gamma_0/2\gamma_m + 1 + \kappa}. \quad (60)$$

It follows from Eq. (60) that, in the high saturation regime, the amplitude of the dip decreases as $1/|V_{21}^{s1}|^4$. The function α_a has an extremum at the point

$$\kappa_e = \frac{\gamma_0/2\gamma_m + 1}{4} \left(\sqrt{1 + 8(\gamma_0/2\gamma_m + 1)^{-1}} - 1 \right). \quad (61)$$

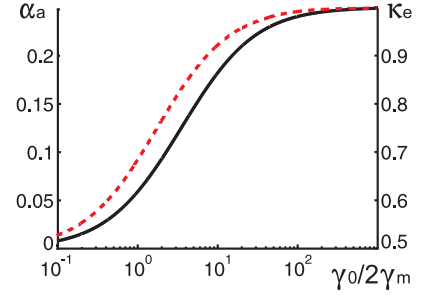


FIG. 2: The extremum point κ_e (black line) and dip amplitude at this point $\alpha_a(\kappa_e)$ (red line) as a function of $\gamma_0/2\gamma_m$.

For the case in which $\gamma_0 \gg \gamma_m$ it is easy to show that the maximum amplitude of the dip $\alpha_a = 0.25$ is obtained at the point $\kappa_e = 1$ [12], but in the general situation there is no simple expression so that a graphical representation is required (see Fig. 2). It can be seen from Fig. 2 that with decreasing γ_0/γ_m the maximal achievable dip amplitude decreases.

IV. NUMERICAL RESULTS

In this section we numerically analyze the absorption spectrum of a weak probe field at the frequency ω_{p1} that scans the TLS (Fig.1). The TLS is driven by two pump fields that are symmetrically detuned from resonance ($\Delta = 0$). Also we consider the case when there can be an additional weak field whose detuning is symmetrically displaced from resonance with respect to the first probe [see Eq. (13)]. In this case, we demonstrate strong parametric interaction between the weak fields in the presence of the pumps. As we mentioned in the previous sections, the branching ratio of γ_{21} , the decay rate from the excited to the ground state, to γ_0 , the decay rate from the excited to the metastable state, plays an important role in the properties of the CPO. We therefore analyze two cases numerically: $\gamma_2 \approx \gamma_0 \gg \gamma_m$ and $\gamma_2 \gg \gamma_0 \approx \gamma_m$.

A. Case 1 $\gamma_2 \approx \gamma_0 \gg \gamma_m$

This range of values for the relaxation constants has been considered in our previous work on CPO [12–15]. However, here two strong pump fields are applied to the same transition. So, instead one CPO resonance in the probe spectrum, we obtain two CPO dips centered at the pump frequencies $w = \pm\delta$ (Fig. 3). According to Eq. (58), increasing the pump Rabi frequencies leads to considerable power broadening of the CPO resonances [Fig. 3(b)]. The bandwidth of the CPO resonances estimated from the numerical simulation is well described by Eq. (58) which was derived for the case in which there is only one strong field [16]. The behavior of each of

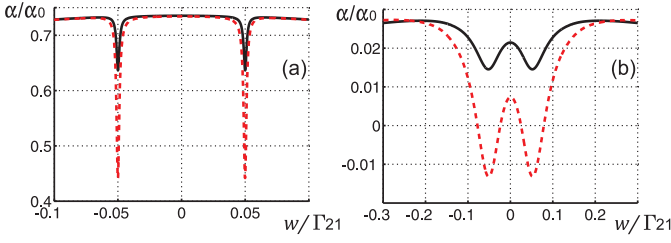


FIG. 3: The spectrum of the probe absorption as the function of the detuning w . $\Delta = 0$, $\delta/\Gamma_{21} = 0.05$, $\gamma_o/\gamma_2 = 0.9$, $\gamma_{21}/\gamma_2 = 0.1$, $\gamma_m/\Gamma_{21} = 10^{-3}$, $\gamma_2/\Gamma_{21} = 2$, $V^{p1} \ll \Gamma_{21}$. a) $V^{s1}/\Gamma_{21} = V^{s2}/\Gamma_{21} = 0.01$ ($\kappa = 0.36$). b) $V^{s1}/\Gamma_{21} = V^{s2}/\Gamma_{21} = 0.1$ ($\kappa = 34$). $V^{p2} = 0$ black line. $V^{p2}/V^{p1} = 2$ red line.

these two resonances appears to be independent - while the probe field is in the region of the CPO resonance created by the first pump, it does not experience any coherent effects that come from the second pump field. The situation became quite different when we add a second symmetrically displaced weak field [Fig. 3 (red dashed lines)]. In the presence of the second weak field, FWM occurs. Due to the effect of the FWM, the absorption of two photons from the pump fields at the frequencies ω_{s1} and ω_{s2} leads to the generation of two photons at the probe frequencies ω_{p1} and ω_{p2} . As a result, the dips in Fig. 3(a) get deeper and there is even amplification of the probe in Fig. 3(b).

The effect of FWM between two weak probes and two pump fields exists (see red dashed lines in Fig. 3) even when the pump Rabi frequencies are well below the transverse relaxation rate Γ_{21} . The amplitudes of the two probes in Fig. 3 are chosen to be unequal in order to obtain a more pronounced effect than in the spectrum of a single probe [12].

In the present case there are no CPO resonances at the subharmonic frequencies $w = \pm(2n+1)\delta$. This is due to the large difference in the saturation parameters for the TLS in the presence and absence of the intermediate state, as shown in Eq. (49). Thus, when the Rabi frequencies are close to the transverse relaxation rate of the TLS where the higher-order nonlinear wave mixing appears [11], the CPO resonances get very broad [see Eq. (58)] and completely disappear.

B. Case 2 $\gamma_2 \gg \gamma_o \approx \gamma_m$

In this range of relaxation parameters, almost all the population decays directly from the excited to the ground state and only a tiny amount decays via the metastable state. In this case, the two CPO resonances centered at the pump frequencies are still observed but their amplitudes get much smaller (compare Figs. 3 and 4). The special feature in this case is that κ and κ_{TLS} are of the same order [see Eq. (49)] so that the CPO resonances

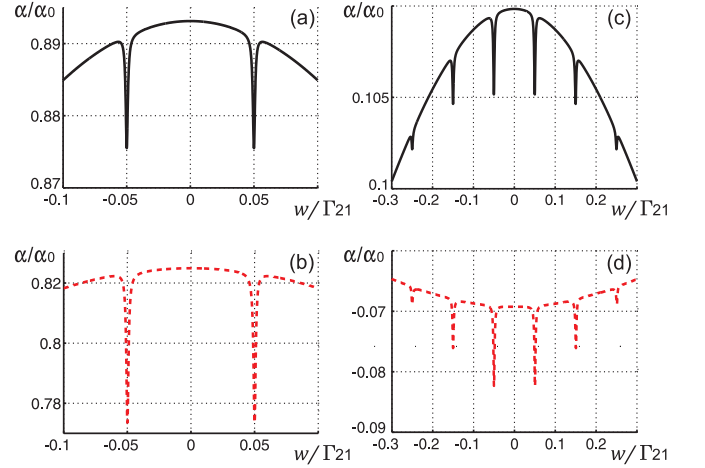


FIG. 4: The spectrum of the probe absorption as the function of the detuning w . $\Delta = 0$, $\delta/\Gamma_{21} = 0.05$, $\gamma_o/\gamma_2 = 10^{-3}$, $\gamma_{21}/\gamma_2 = 0.999$, $\gamma_m/\Gamma_{21} = 10^{-3}$, $\gamma_2/\Gamma_{21} = 2$, $V^{p1} \ll \Gamma_{21}$. When the pump Rabi frequencies are much smaller than a transverse relaxation rate $V^{s1}/\Gamma_{21} = V^{s2}/\Gamma_{21} = 0.1$ ($\kappa = 0.08$) there are only two CPO resonances a,b) and the resonances at the subharmonics appears when the pump Rabi frequencies are increased $V^{s1}/\Gamma_{21} = V^{s2}/\Gamma_{21} = 1$ ($\kappa = 4$) c,d). The presence of the second probe $V^{p2}/V^{p1} = 2$ demonstrate the parametric interaction between the weak fields b,d) ($V^{p2} = 0$ for a,c)).

do not experience much power broadening [see Eq. (59)]. These facts allow one to combine the effect of the higher-order wave mixing which appears at pump Rabi frequencies comparable with the transverse relaxation rate Γ_{21} [11] and the existence of narrowband CPO resonances. In Figs. 4(c) and (d), the existence of the CPO resonances at the subharmonic frequencies $w = \pm(2n+1)\delta$ where $n = 0, 1, 2, 3, \dots$ is clearly seen. For example the resonance that is located at the $w/\Gamma_{21} = 0.15$ ($n = 1$) on the Fig. 4(c) corresponds to the process of the three-wave mixing between pump fields $\omega_{sub,0.15} = 2\omega_{s1} - \omega_{s2}$. In this case, as in the previous one, there is strong parametric interaction between the weak symmetrically displaced fields [Fig. 4(b) and (d)]. In addition, the pump Rabi frequencies are of the same order as the transverse relaxation rate. This leads to parametric interaction between the weak fields not only in the CPO region, as in the previous case, but in a broad spectral range, as shown in Fig. 4(d) [17].

V. CONCLUSION

In summary, we have demonstrated the appearance of narrowband CPO responses at frequencies shifted from the pump frequency. The new CPO resonances appears at the frequencies $\omega_{sub} = \omega_0 \pm (2n+1)\delta$ due to multiphoton mixing between components of the bichromatic pump. We expect that these spectral features will al-

low spectral filtration of the signal field from the strong pump in experiments with slow light, and biphoton generation based on the effect of CPO. Also, in the region of the CPO dip there is effective parametric interaction between probe fields for both the cases considered in Sec. IV. The subharmonic resonances that appear when the condition $\gamma_2 \gg \gamma_o \approx \gamma_m$ is satisfied can be investigated in atomic TLS systems where the decay via dipole-forbidden transitions are taken into account, and in certain NV centers in diamond [18]. In addition, the predicted sub-

harmonic CPO resonances may have contributions to the resonances observed in the recent experiment [19] where the was driven by a bichromatic pump.

Acknowledgments

A. V. S. was supported by RFBR 12-02-31621

-
- [1] M. Fleischhauer, A. Imamoglu, and J. P. Marangos, Rev. Mod. Phys. **77**, 633 (2005).
 - [2] E. V. Baklanov and V. P. Chebotaev, Sov. Phys. JETP **33**, 300 (1971); M. Sargent III, Phys. Rep. **43**, 223 (1978); R. W. Boyd and M. Sargent III, J. Opt. Soc. Am. B **5**, 99 (1988).
 - [3] S. E. Harris, J. E. Field, and A. Kasapi, Phys. Rev. A **46**, R29 (1992).
 - [4] M. S. Bigelow, N. N. Lepeshkin, and R. W. Boyd, Science **301**, 200, (2003).
 - [5] H. Friedmann, A. D. Wilson-Gordon, and M. Rosenbluh, Phys. Rev. A **33**, 1783 (1986).
 - [6] V. Balic, D. A. Braje, P. Kolchin, G. Y. Yin, and S. E. Harris, Phys. Rev. Lett. **94**, 183601 (2005); P. Kolchin, S. Du, C. Belthangady, G. Y. Yin, and S. E. Harris, Phys. Rev. Lett. **97**, 113602 (2006); S. Du, P. Kolchin, C. Belthangady, G. Y. Yin, and S. E. Harris, Phys. Rev. Lett. **100**, 183603 (2008).
 - [7] C. H. van der Wal, M. D. Eisaman, A. Andre, R. L. Walsworth, D. F. Phillips, A. S. Zibrov, and M. D. Lukin, Science **301**, 196 (2003); A. Kuzmich, W. P. Bowen, A. D. Boozer, A. Boca, C. W. Chou, L.-M. Duan and H. J. Kimble, Nature (London) **423**, 731 (2003); J.K. Thompson, J. Simon, H. Loh, and V. Vuletic, Science **313**, 74 (2006); S. Du, J. Wen, and M. Rubin, J. Opt. Soc. Am. B **12**, C98 (2008).
 - [8] A. V. Sharypov and A. D. Wilson-Gordon, Phys. Rev. A **84**, 033845 (2011).
 - [9] Z. Ficek and H. S. Freedhoff, Spectroscopy in polychromatic fields. Progress in Optics **40**, 389 (2000).
 - [10] Y. Zhu, Q. Wu, A. Lezama, D. J. Gauthier, and T. W. Mossberg, Phys. Rev. A **41**, 6574 (1990).
 - [11] Z. Ficek and H. S. Freedhoff, Phys. Rev. A **48**, 3092 (1993).
 - [12] A. V. Sharypov, A. Eilam, A. D. Wilson-Gordon, and H. Friedmann, Phys. Rev. A **81**, 013829 (2010).
 - [13] I. Azuri, A. Eilam, A.V. Sharypov, A. D. Wilson-Gordon, and H. Friedmann, Optics Communication **283**, 4318 (2010).
 - [14] A. Eilam, I. Azuri, A. V. Sharypov, A. D. Wilson-Gordon, and H. Friedmann, Opt. Lett. **35**, 772 (2010).
 - [15] Yu. I. Heller and A. V. Sharypov Opt. Spectra **106**, 252 (2009).
 - [16] The values of κ given in the captions of Figs. 3 and 4 are found under the assumption that the population inversion can always be written in the form of Eq. (48) where $\sigma_0^{0,0}$ (zero-order population inversion) is found from the numerical solution.
 - [17] R. W. Boyd, M. G. Raymer, P. Narum, and D. J. Harter, Phys. Rev. A **24**, 411, (1981).
 - [18] J.M. Smith, F. Grazioso, B.R. Patton, P.R. Dolan, M.L. Markham and D.J. Twitchen, New J. Phys. **13**, 045005 (2011).
 - [19] A. M. Akulshin, R. J. McLean, A. I. Sidorov and P. Hannaford, J. Phys. B: At. Mol. Opt. Phys. **44**, 175502 (2011).